6-2003

AFCI Quarterly Input – UNLV April through June, 2003

Harry Reid Center for Environmental Studies. Nuclear Science and Technology Division

AFCI Quarterly Input – UNLV
April through June, 2003

1.0 University of Nevada, Las Vegas (UNLV)

UNLV Transmutation Research Program. The University of Nevada, Las Vegas supports the AFCI through research and development of technologies for economic and environmentally sound refinement of spent nuclear fuel. The UNLV program has four components: infrastructure, international collaboration, student-based research, and management and program support.

1.1 Infrastructure Augmentation

1.1.1 Infrastructure Augmentation Scope

The infrastructure augmentation component of the UNLV Transmutation Research Program enhances UNLV's research staff, facilities, and academic programs to increase the ability of the university to perform AFCI research.

1.1.2 Infrastructure Augmentation Highlights

- **Ph.D. Program in Radiochemistry**. UNLV approved a proposal for a new Radiochemistry graduate program on April 28, 2003. The proposal was submitted to the Board of Regents of the University and Community College System of Nevada on June 18, 2003. The Board of Regents should address the proposal at their next meeting in August. If approved, the program will officially start fall term 2004. However, students may start coursework in fall term 2003. The program will be a joint program between the Department of Chemistry and the Department of Health Physics and will be governed by the Graduate College.
- **Chemistry Professorship**. UNLV made an offer on two tenure-track associate professorships in the Department of Chemistry in the following areas: Materials Chemistry and Actinide Chemistry. These positions will be supported 49% by the UNLV Transmutation Research Program.
- **Facilities Progress Update**. Three facilities are in the laboratory remodeling stage: the Transmission Electron Microscope user facility, the Interim Lead-Bismuth Eutectic Loop facility, and the Inductively Coupled Plasma Atomic Emission Spectrometer user facility. Architectural and engineering drawings have been completed for the remodeling. The contractor bids for the TEM and LBE facilities were opened this quarter and work is scheduled to be completed by the end of next quarter. The ICP AES has arrived at UNLV and is awaiting installation after minor room modifications. It is expected to be operational by next quarter.

1.2 International Collaboration

1.2.1 International Collaboration Scope

The international collaboration component of the UNLV Transmutation Research Program enhances UNLV's breadth of scientific and scholastic experience. University collaboration is also an efficient conduit for international collaboration that benefits the national AFCI program.

UNLV has ongoing relationships with the Khlopin Radium Institute (KRI) in St. Petersburg, Russia; the Institute for Physics and Power Engineering (IPPE) in Obninsk, Russia; and members of the International Molten Metal Advisory Committee (from Sweden, Germany, Belgium, and Italy).

1.2.2 International Collaboration Highlights

- **International Science and Technology Center (ISTC)**. The agreements and contracts to extend the collaboration with the Institute of Physics and Power Engineering, LANL, and UNLV over the ISTC Target Complex 1 located at UNLV are being drafted and are expected to be finalized and signed next quarter.
- **Khlopin Radium Institute**. Tax payment issues were resolved regarding the three KRI contracts and payments have been processed. The KRI-built He-3 neutron detector is in transit to UNLV and is expected to be tested at the end of July 2003 (see Task 6 in Student Research section) which will complete the project. The other two projects support Student Research Task 15 (Iodine Sequestration) and Task 16 (Fluorapatite Waste Forms). See their respective tasks in the next section for more information.

1.3 Student Research

1.3.1 Student Research Scope

The Student Research component is the core of the UNLV Transmutation Research Program with steadily increasing funds as the program evolves and capability expands. The milestones, schedules, and deliverables of the student research projects are detailed in the individual research proposals. UNLV currently has 16 student research tasks that include 37 graduate students and involve 33 faculty members. The tasks are divided below in terms of their research area: fuels, separations, and transmutation sciences.

1.3.2 Student Research Highlights

Metallic Fuel Pins (Task 1) Highlights.

- The impact of mold preheat temperature and fuel pin diameter on the ability of copper and stainless steel molds to solidify all the molten material for 0.5 m fuel pin have been evaluated.
- The solidification processes of constant inlet velocity and constant pressure have been studied by using different molds preheated temperature, and different inlet pressure.
- The numerical model for the upper part of the casting furnace that includes the crucible and coils has been set up. The governing equations for the induction heating modeling have also been studied and developed.
- The change of the average filling velocity during the solidification process in the molds for different convection heat transfer coefficients was analyzed.
- The impact of the convection heat transfer coefficient on the melt solidification process was studied by using the different convection heat transfer coefficient values of h.
- FIDAP was used to solve the induction heating model with six governing equations which can calculate the power deposition rate in the crucible.
- The overall mass transfer coefficient of americium in the crucible was studied.

Remote Fuel Fabrication (Task 9) Highlights.

- Graduate student Richard Silva continued the development of a simulation model with a Waelischmiller hot cell robot. He will continue to develop detailed 3-D process simulation models as his M.Sc. thesis project.
- Ph.D. student Jae-Kyu Lee continued his research on Concepts and Methods for Vision-Based Hot Cell Supervision and Control, focusing on rule-based object recognition.
- Undergraduate student Jamil Renno developed better control algorithms, and created simulations of pick and place actions for the hot cell manipulator.

Systems Engineering Model (Task 8) Highlights.

- The Graphical User Interfaces (GUI's) for the aqueous input stream and the organic input stream were developed.
- The Active X technique from the Visual Basic program was successfully used and developed to run the instance of MATLAB and execute MATLAB function and export the result back to the main GUI.
- An Object Oriented Programming (OOP) approach has been developed and implemented for the final three sections of the new modeling approach (First, Intermediate, and Last sections).
- A number of AMUSE analyses were conducted to demonstrate the ability of the code to store the data, plot the data, and to obtain feedback from ANL on how to improve the interface.
- The AMUSE code can now be called from within MATLAB as part of the Systems Engineering Modeling effort.
- Input files and results files can be successfully generated for individual runs and for multiple runs through MATLAB calls. Refinements will be made to this approach to allow for more runs and to allow for optimization.

Criticality and Heat Transfer Analyses of Separations Processes (Task 11) Highlights.

- Research initiated to develop and evaluate criteria for the use of commercial dry storage casks for strontium and cesium storage.
- Graduate student Elizabeth Bakker is an intern at Argonne National Laboratory for the summer.
- Initiated research on the GUBKA process of containing radioactive waste.
- Further research is being conducted into cesium/strontium storage forms.
- Continued investigation of criticality tendencies of mixtures of americium and curium metal.
- Continued investigation of criticality tendencies of mixtures of americium oxide and curium oxide.
- Performed literature searches for necessary properties of cesium oxide and strontium oxide.

Immobilization of Fission Iodine (Task 15) Highlights.

- Literature Search: We are continuing to search the chemical literature for references relevant to immobilization of iodine.

- Preparation of Test Fullerene-containing Carbon Compounds (FCC) and NOM (natural occurring material): We are conducting experiments primarily with sphagnum peat moss and a commercial lignin preparation at this time. We have not received any FCC preparations from KRI. We have obtained a commercially available fullerene preparation from Aldrich and we will conduct some experiments with this material in preparation for the FCC studies.
- Analytical Methods Testing: We have established our primary analytical methods for iodide, iodine and iodate. We are establishing method for volatile iodine species formed by reaction with NOM and by pyrolysis of NOM.
- Set up Experimental Apparatus: The iodine generator is complete and undergoing testing. We have made some additional modifications of the device that should substantially improve reproducibility. We have constructed a device for simulating fuel dissolution and we are performing some preliminary tests.
- Iodine Binding Experiments (FCC): We have not received any materials for testing at this time. We have obtained what we believe to be analogous material from Aldrich Chemical, and will conduct some preliminary tests with this material.
- Iodine Binding Experiments (NOM): We are continuing experiments with sphagnum peat moss and have collected additional data on sequestration of iodine from the vapor phase. We are examining the effect of flow rate and nitric acid fumes on recovery of iodine.

Fluorapatite Waste Forms (Task 16) Highlights.

- Baseline spectroscopic measurements have been obtained for commercial hydroxyapatite and natural fluorapatite using a wide variety of techniques (*e.g.*, Raman, XPS, FT-IR) useful for probing the chemical and physical properties of materials.
- Detailed SEM images of natural fluorapatite crystals indicate the presence of naturally included minerals (*e.g.*, Ni), offering the possibility of studying natural analogs to waste-loaded apatite materials.

Niobium Cavity Fabrication Optimization (Task 2) Highlights.

- Calculation regarding the spatial resolution needed for Secondary Electron Emission (SEE) experiments have been performed. This will determine the type of position sensor technology needed for experimentation.
- Some initial flow visualization studies have begun. Gravitational forces appear to be more significant than flow forces causing the dye to diffuse into the mainstream too fast.
- Track 5.0 (electromagnetic particle tracking program) was employed to study a more realistic sensor geometry as is available on the market.

LBE Corrosion of Steel (Task 3) Highlights.

- Collaboration with X-ray microscopy group at Lawrence Livermore National Laboratory initiated.
- 316 and 316L samples exposed to LBE in Russia were previously thought to have had different carbon content, based on Russian analysis. In May, it was found that the carbon content is about the same in the two samples, and that differences should be attributed to surface preparation: cold-rolled vs. annealed.

- A Raman spectrum from a steel sample exposed to LBE was successfully obtained. Previously Raman data was obtained only from standards. This is an important step forward.

Environment-induced Degradation of Materials (Task 4) Highlights:

- C-ring and U-bend specimens of Alloys HT-9 and EP-823 have been machined. A part of these specimens has been sent to LANL for Stress Corrosion Cracking (SCC) testing in molten LBE environment. Simultaneously, SCC testing in aqueous solutions has been initiated at the MPL using these types of self-loaded specimens.
- A significant number of SCC tests using calibrated proof rings and smooth tensile specimens of martensitic Type 422 stainless steel, and Alloys EP-823 and HT-9 has been completed in both neutral and acidic aqueous environments under constant-load conditions at ambient and elevated temperatures. No failure has been observed with Alloy EP-823 and Type 422 stainless steel in the neutral solution at either temperature. However, failures were observed with these two alloys in the acidic solution at 90^{o}C. For Alloy HT-9, failures were observed in both environments at 90^{o}C. Additional tests are ongoing using notched tensile specimens.
- SCC testing using slow-strain-rate technique has been completed in both environments at ambient and elevated (60 and 90^{o}C) temperatures involving smooth and notched tensile specimens of all three martensitic alloys. Results indicate that, as anticipated, the time to failure and the true fracture stress were gradually reduced with smooth specimens at increased testing temperatures and a lower pH value. However, in the presence of a notch, the true fracture stress was enhanced due to a smaller area at the root of the notch. As expected, the ductility parameters (% elongation and % reduction in area) were also substantially reduced due to the combined effect of elevated temperatures and an acidic pH.
- Fractographic evaluations of the primary fracture faces of the tested tensile specimens by SEM revealed a combination of ductile, and brittle failures (intergranular and transgranular). Metallographic evaluations of the broken specimens by optical microscopy revealed secondary cracks along the gage section showing branching at the bottom of these cracks. Metallographic studies are ongoing.
- Electrochemical polarization studies to evaluate the localized corrosion behavior of all three alloys are ongoing. The preliminary data indicate that the corrosion potential and the critical pitting potential became more active (negative) with increasing temperature and reduced pH of the test solution, as expected.

LBE Corrosion Modeling (Task 5) Highlights:

- Mesh independence runs are being tested to find out the smallest possible number of nodes to be used in the CFD runs that maintain a certain accuracy level.
- Some results are sought for refinements of 3-D simulation runs for a closed loop. These refinements are mainly in the elbow flow areas.
- Sudden expansion 2-D runs are being performed with the need to track the behavior of concentration values for several modes close to the surface so that a time-averaged concentration value can be calculated from which a flux gradient of concentrations can be made.

- "Grid independence" has been determined for our laminar and turbulent flow runs and the researchers have started to make several runs for different flow, and temperature conditions related to the LANL lead-bismuth Delta loop.

Neutron Multiplicity (Task 6) Highlights:

- ^{3}He Neutron Multiplicity detector prototype (64 element) is completed and will be delivered to UNLV next quarter.
- The 304 Stainless Steel stand needed to support the ^{3}He detector system was completed in mid-May subsequent to technical drawings being transferred, approved at KRI and at HRC, and then fabricated in Oak Ridge, TN.
- Nuclear Transport Code Models (MCNP 4B, MCNPX) that were needed to finalize the ^{6}Li glass fiber neutron multiplicity detector prototype design were verified at UNLV and also with independent models completed by Dr. Richard Craig (at PNNL). Lead target configuration for the ^{3}He system was computationally changed to that of a rectangular block target and additional MNCPX models were constructed for this target/detector geometry.
- Finalized the graphical depiction of the results of nuclear transport models for the neutron production source volume and neutron capture efficiencies of specific elements of the KRI ^{3}He 60 element detector systems. The target in these models was modified from the AS1 configuration (cylindrical) to rectangular targets. Transport code models of rectangular targets are now being constructed.
- The glass fiber neutron multiplicity detector prototype (^{6}Li glass fiber detector) is approximately 90% complete for all hardware and electronic card production (for optoelectronic interfaces, light guides, signal train, firmware). Cabling and stand-off electronics shielding has yet to be completed.

Dose Conversion Coefficients (Task 7) Highlights:

- Completed the dose coefficients calculations for the quality assurance (QA) radionuclides.
- Implemented the new EDISTR computer code.
- Reclassified radionuclides into categories that can produce dose coefficients.
- Four dose coefficients from the Category 1 radionuclides were completed, which leaves about 6 more.
- Literature search for nuclear data bases for the Category 2 radionuclides continued.
- Calculates of dose coefficients completed for the Category 1 radionuclides which have complete ENSDF files.

Properties of Alloy EP-823 (Task 10) Highlights:

- The Materials Testing System (MTS) machine to perform tensile testing has been modified to accommodate high-temperature testing in the presence of an inert gas (nitrogen) using a custom-made chamber. The testing temperature using this hot chamber can be monitored by two K-type thermocouples.
- A laser extensometer having a scan rate of 100 scans/second has also been added to this MTS unit to measure the elongation in the gage section of test specimen during the plastic deformation under tensile loading at the desired strain rate.

- A pair of custom-built water-cooled specimen grips made of maraging steel (M250) has been attached to the MTS machine to prevent these grips from being heated during high-temperature testing.
- Testing has been performed at ambient temperature and 100^{o}C using tensile specimens fabricated from vacuum-melted and heat-treated (at the Timken Company, OH) bars of martensitic Alloy EP-823. Preliminary data indicate that both the yield strength (YS) and the ultimate tensile strength (UTS) of the tested material were slightly reduced at the elevated temperature. However, no significant reduction in ductility in terms of percent elongation (%El) and percent reduction in area (%RA) was observed in these tests.
- Temperature profiles have been developed to determine the times needed to achieve the desired test temperature, as a part of the furnace calibration process. Tests are in progress.

Radiation Transport Modeling of Beam-Target Experiments (Task 12) Highlights:

- Parallelization of MCNPX for a Parallel Virtual Machine (PVM) complete. Working on Message Passing Interface (MPI) bugs and compiling problems.
- Writing a program to convert CAD files, more specifically IGES types, into a textual input deck to run in Monte Carlo programs.
- Analysis of linearization characteristics on Beowulf cluster complete. Now working on characteristics of the Supercomputing Center and the linearization of criticality studies.
- Continued benchmarking on shared memory systems and Beowulf cluster. Testing between MPI versions and PVM. MPI seems to be outperforming PVM by a factor of three on the Beowulf cluster. Runs are currently being conducted on the shared memory systems.
- The new machines are AMD 2400's while the older slave machine were AMD 2000's. A program is being made that can look at a cluster and determine the CPU speeds of each computer. Then, the master can determine from this information how large of a job each slave machine should receive.

Oxygen Sensing in LBE (Task 13) Highlights:

- Testing of the LabView module for our apparatus was performed.
- Performed electrical test on the DC motor for our apparatus.
- The control plan using LabView for the apparatus was revised.
- Two graduate students will be sent to LANL to work on the project once their security clearance has been approved.
- The assembly of the apparatus has almost been completed. It may be shipped to LANL by the end of the summer.
- Some preliminary 3-D simulation results have been obtained for a simplified model.

Positron Annihilation Spectroscopy (Task 14) Highlights:

- Cold-worked (7 and 11%), three-point-bent (TPB), and welded (similar and dissimilar alloys) specimens of martensitic Alloy EP-823, and austenitic Type 304L stainless steel have been fabricated, and subjected to residual stress measurements by X-ray Diffraction (XRD), Positron Annihilation Spectroscopy (PAS) and ring-core methods. Residual stress measurements by neutron diffraction have not yet been initiated.

- PAS method has been used at the Idaho State University to determine the residual stresses in cold-worked and TPB specimens of both Alloy EP-823 and Type 304L stainless steel. The resultant data have been analyzed in terms of either S or T parameter.
- XRD measurements have been performed on TPB specimens of Alloy EP-823 at the Lambda Research Laboratory (LRL), Cincinnati, OH. Similar measurements could not be performed on Type 304L stainless steel due to its course-grained structure. Ring-core method has been applied at the LRL to measure residual stresses at various locations (fusion-line, base metal and heat-affected-zone) of the welded specimens consisting of similar and dissimilar alloys (304L/304L, EP-823/EP-823, and 304L/EP-823).
- The comprehensive test data are currently being analyzed in collaboration with all three participating testing laboratories (MPL, ISU and LRL). Simultaneously, contacts have been made with the Atomic Energy of Canada Limited (AECL) to measure residual stresses in different types of specimens by neutron diffraction technique.
- Metallurgical characterizations including tensile properties, hardness and microstructural evaluation are in progress at the UNLV Materials Performance Laboratory.

1.3.3 Student Research Technical Summary

FUELS TECHNOLOGY

Metallic Fuel Pins (Task 1). Progress continues on the analysis of casting and solidification of the melt into molds. Modeling results for constant pressure casting, which is more realistic, have been obtained and produce physically realistic results for flow that starts, flows, and then eventually stops as it enters the mold. Potential mass transfer modeling features (Lammuir's law for example) are being studied to enhance the capabilities of a mass transfer in a detailed system model. Different parameters are being varied as part of a parametric study to evaluate factors that impact the flow of the melt into the molds. The ability to include the induction heating governing equations as part of an overall system model is being studied and preliminary efforts to include this complex phenomenon as part of a more detailed model are underway.

The impact of mold preheat temperature and fuel pin diameter on the ability of copper and stainless steel mold to solidify all the molten material for 0.5 m fuel pin have been evaluated. The solidification processes of constant inlet velocity and constant pressure have also been studied by using different molds preheated temperature, and different inlet pressure.

We have also set up the numerical model for the upper part of the casting furnace that includes the crucible and coils. The governing equations for the induction heating modeling have also been studied and developed. FIDAP was used to solve the induction heating governing equations in order to find the solution of the power deposition rate in the crucible.

The changes of the average filling velocity during the solidification process in the molds for different convection heat transfer coefficient have also been analyzed. The solidification process is analyzed at constant filling pressure, P=20 kPa. All the other physical properties, initial and boundary conditions are kept as constants. For example, the material of the mold is copper, the mold preheated temperature is 400 ^{o}C, initial melt temperature is 1500^{o}C. The average filling velocity increases rapidly at the beginning of the solidification process till it reaches the maximum value. And then it decreases to zero when the melt is solidified at the centerline of the

mold. It is also shown that the entire solidification process with the higher of h value is faster than the lower one. And the minimum of average filling velocity can be found at the highest of h value.

The impact of the convection heat transfer coefficient on the melt solidification process is also studied by using the different convection heat transfer coefficient values of h. The melt solidification process time along with the radial location and the different values of h are shown as follow. When the diameter of solidified melt reaches roughly 25 percent of the outer diameter, the melt is quickly solidified and the flow is stopped. Then the slow cooling process is occurred after this specific time because the conduction is predominant compared to the mixed of convection and convection process before the solidification completed. Comparison of solidification process for different mold material for T=800^{o}C is shown in Figure 1.3.1.

At the beginning of the process, the material in the glass quartz mold is solidified slower than that in the stainless steel mold and copper mold. This is because the thermal conductivity of glass quartz is much smaller than copper and stainless steel.

For the stainless steel mold and copper mold, the average velocity reaches to the maximum velocity and then drops to zero quickly compared to the glass quartz mold. However, for the glass quartz mold, the average velocity reaches to the maximum velocity is slower and it stays at the maximum value range for a longer time, and then drops down slowly. It is because the material of glass quartz has a much smaller value of thermal conductivity than that of copper and stainless steel. It is easy to understand that it takes a longer time for the glass quartz mold for the whole solidification process.

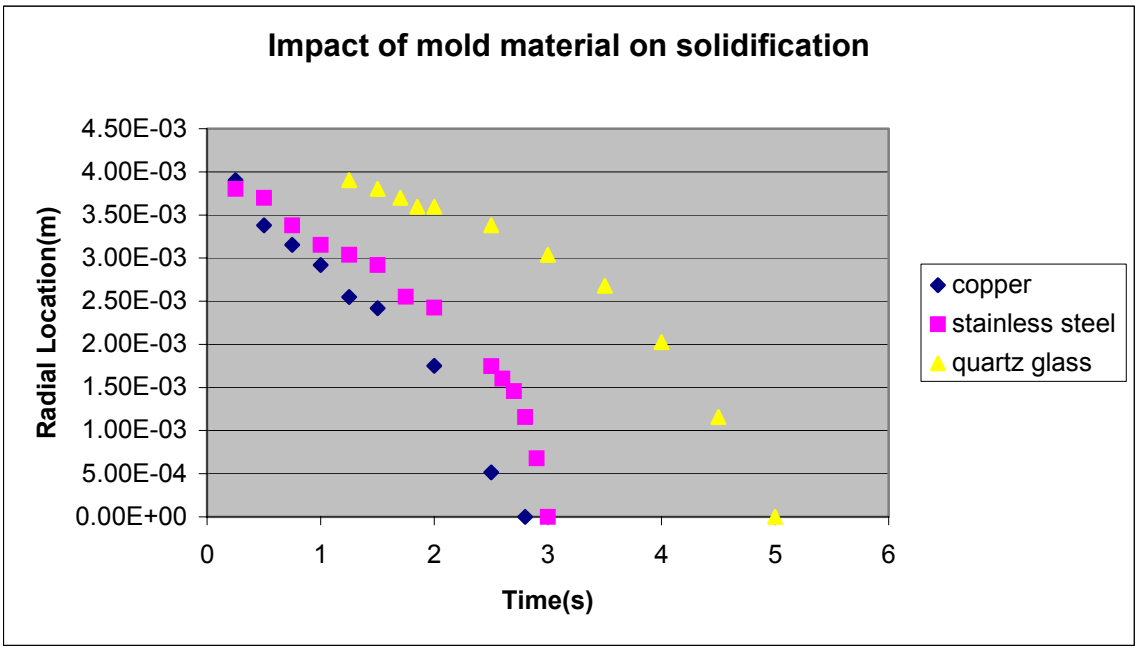

Figure 1.3.1. Comparison of solidification process for different mold material

Boundary conditions and initial conditions: inlet pressure: P= 20 kPa; inlet temperature= 1500 ^{o}C; mold preheated temperature: T=800 ^{o}C; convection heat transfer coefficient h=2000 W/m^{2} ^{o}C; phase change temperature: 1400-1410 ^{o}C

Remote Fuel Fabrication (Task 9). The objective of this project is the design and evaluation of manufacturing processes for AFCI fuel fabrication. The large-scale deployment of remote fabrication and refabrication processes will be required for all transmutation scenarios. The evaluation of the fabrication processes will create a decision support data base to document design, operations, and costs. Fabrication processes required for different fuel types differ in terms of equipment types, throughput, and cost. Differential cost Implications of various fuel choices will be assessed. Another aspect is the assessment of robotic technology and robot supervision and control, and the simulation of material handling operations using 3-D simulation tools with view towards the development of a fully automated and reliable, autonomous manufacturing process. Such development has the potential to decrease the cost of remote fuel fabrication and to make transmutation a more economically viable process. An added benefit would be the potential for large reductions in dose to workers. This project is being conducted in close cooperation with the fabrication development group at Argonne National Lab.

Manufacturing processes will be simulated as robotic operations supervised by remote operators. Both normal operations as well as failure scenarios will be investigated, analyzed, and simulated. The results of the simulations will be used by AFCI program personnel to perform sensitivity studies on the impact of different fuel types on system operation. Conceptual designs for plant designs and the accompanying supervision and control systems will be developed. Impacts on transmutation system capital cost, economics of operation, estimates of process loss, and environmental and safety issues will be estimated.

During the present reporting period, the robot simulation model for robot control under Matlab Control software was improved further. Matlab controls the spatial robot model, comprising a geometric model as well as the robot dynamics. Thus a realistic simulation of the forces and torques present during robot motion is being generated. The fuzzy logic controller used during the previous quarter was replaced by a set of six PID controllers. The design parameters of each controller were optimized for minimum overshoot. Care was taken to avoid arm oscillations under any circumstances.

An object's surface is characterized by a series of connected points. During the reporting period, we worked on knowledge based methods for the retrieval of stored information and for pattern matching. The relationship between a surface and its stored features is represented as a sequence of connected boundary parts, each of them represented as a sequence of junction types in the connectivity table. A set of initial rules for pattern matching has been developed and verified. Decision functions have been also defined as computer code for implementation and testing. The proper function of the rules was tested on synthetic objects and on photographed overlapping objects. The two objects were photographed using a CCD camera in the robotics lab

SEPARATIONS TECHNOLOGY

Systems Engineering Model (Task 8). The objectives of this task are the development of a systems engineering model and the refinement of the Argonne code AMUSE (Argonne Model for Universal Solvent Extraction). The detailed systems engineering model is the start of an integrated approach to the analysis of the materials separations associated with the AFCI Program. A second portion of the project is to streamline and improve an integral part of the overall systems model, which is the software package AMUSE.

AMUSE analyzes the UREX process and other related solvent extraction processes and defines many of the process streams that are integral to the systems engineering model.
Combining these two tasks is important in ensuring that calculations made in AMUSE are accurately transferred to the overall systems model. Additional modules will be developed to model pyrochemical process operations not treated by AMUSE. These modules will be refined as experiments are conducted and as more knowledge is gained in process steps.

Five specific objects are being implemented for the graphical user interface as a result of the meetings with ANL researchers: Flow sheet, Section, Streams, Stages and Concentrations. Work continues on the development of flow sheet objects that allows the user to select flow sheet name, reports location, type of process and other required input.

A Separations area called "Tools" is being developed to allow the user to develop process blocks within the software environment to build a specific process flow sheet, which includes the ability to generate process streams, sections, stages and input data for each of them. Development of an overall process model continues using MATLAB with SIMULINK that will eventually allow the top five most influential factors to the process to be automatically selected those factors will be used for the design variables for the optimization. The interface has been changed to implement the Object Oriented Programming (OOP) approach. With this approach our interface will be able to do all operations as done in AMUSE. Based on the following constraints we have developed three user controls to define the flow sheet:

- All the sections should have a section name and number of stages.
- First section should have both aqueous and organic streams.
- Aqueous feed is mandatory to all sections.
- Stage Sampling and Stage Specific Input can be given to any section.
- Last section should have organic stream.
- First section should have aqueous effluent as output
- Last Section should have Organic Effluent as output.

The flowsheet object is an integration of different objects. We have section, stage, aqueous and organic streams and aqueous and organic feeds as objects. Events are written for each object to give input. For this a number of forms are created which takes input. The main form will have flowsheet object and tools to create the flow sheet and to give input. Connectors are removed because by default the streams go from one block to the consecutive block. The drag and drop mechanism is now implemented only for last section. The user now clicks on each object to give input.

We have successfully used and developed the Active X technique from Visual Basic program to run the instance of MATLAB and execute MATLAB function and export the result back to the

main GUI. We have also successfully developed the ability to open Excel application programs, add workbooks, and change active worksheets by using ActiveX automation technique from MATLAB program.

Criticality and Heat Transfer Analyses of Separations Processes (Task 11). The success of the AFCI program will rely upon the ability of radiochemists to separate spent nuclear fuel. The Chemical Technology Division at Argonne National Laboratory is actively involved in the development of pyrochemical separation technology that minimizes the usage of strong acids with the subsequent problems involved in disposing of the acidic residue.

Small scale experiments are being validated at ANL to separate spent nuclear fuel, but they must be scaled up to accommodate the large amount of commercial spent fuel that must be treated. As the volume of waste to be treated is increased, there is a higher probability that fissionable isotopes of plutonium, americium, and curium can accumulate and form a critical mass. Criticality events can be avoided by ensuring that the effective neutron multiplication factor, k_{eff}, remains below a safe level. NRC regulations normally allow an upper value of 0.95 for k_{eff}. This parameter can be computed for any combination of fuel and geometry using Monte Carlo neutron transport codes. Scale 4.4a from the Oak Ridge National Laboratory and MCNP4C2 from the Los Alamos National Laboratory are two codes that are regularly used to assess criticality.

Immobilization of Fission Iodine (Task 15). The recovery of iodine released during the processing of used nuclear fuel poses a significant challenge to the transmutation of radioactive iodine. This task will develop and examine the use of Fullerene Containing Carbon (FCC) compounds as potential sorbents for iodine release from the reprocessing of nuclear fuel. This work will also include the development of bench-scale testing capabilities at UNLV to allow the testing of the FCC material in a simulated process off-gas environment. This experimental capability will also be used to test other potential sorbtion materials and processes, such as natural organic matter (NOM) and other promising alternatives. This work also examines the development of a process to convert the sorbed iodine into a ceramic material with the potential for use as either a transmutation target or as a waste form in a partitioning and sequestration strategy.
Analytical methods for measuring the speciation of iodine under vapor and aqueous conditions are continuing to be developed.

Ion Chromatography: In the second quarterly report we reported that I^- and IO_3^- have been quantified and separated by ion chromatography on a Dionex AS-9 column. We discovered some interference with this method and have switched to a Novasep A1 anion column (from Alltech Associates) that has been optimized for hydrophobic anions. The new column has resolved the interference problem.

Pyrolysis GC/MS: We have done some experiments with iodinated sphagnum moss and have discovered that during pyrolysis the major iodinated organic compound released is methyl iodide. We are in the process of calibrating this method so that we can quantify the amount of methyl iodide released during pyrolysis. Some additional glassware had to be ordered to this

end. We believe that this process can serve as a basis for concentration iodine from NOM sequestering agents and processing this iodine into a form suitable for accelerator processing.

We are continuing experiments to determine if the formation of volatile iodine species (e.g. iodoform) occurs during the reaction of iodine with Sphagnum peat and alkali lignin. We are optimizing the headspace solid phase micro extraction (SPME) method for iodoform and other volatile iodinated species.

We have conducted additional experiments with the iodine generator. We have examined the effects of nitric acid fumes (at 40^{o}C) on iodine sequestration. Traps were prepared with sphagnum peat and $Ca(OH)_2$ and break through was monitored. Results indicate that at up to 1000 column volumes trapping efficiency for I_2 was greater than 95%.

In Figure 1.3.2 the composite of a number of peat column studies is shown. The fraction of iodine (concentration ~$1.2*10^{-5}$ mol/L) removed from the flowing gas stream is graphed against the number of bed volumes of nitrogen passed through the column. The nitrogen steam was split so that have the flow was saturated with iodine and half with nitric acid. The flow streams were combined and passed though the peat column. Using the criteria of 5% (for break through), it appears that 1000 bed volumes can be passed through these columns under these conditions before the column is effectively exhausted. The column used in this study had a bed volume of 0.9 mL ± 0.1 mL

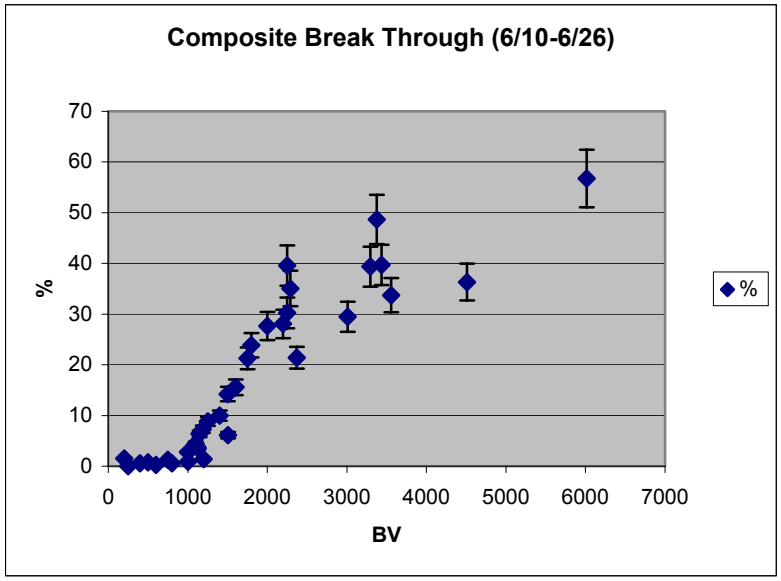

Figure 1.3.2. Percent of iodine in sorbed by Peat columns. The vapor phase was concentration of iodine was $1.2*10^{-5}$ mol/L and was about 50% saturated with nitric acid fumes.

Upon completion of the breakthrough experiment the contents of the column were leached with distilled water (24 hours). The iodide and iodate content of the leachate was measured using ion chromatography. The results of this exercise indicate only a small fraction of the iodine (<10%) was removed by the water leaching leaching. This observation has interesting mechanistic implications that we will continue to investigate.

Investigation of Active Chlorine Resin:

In our previous report we discussed the use of active chlorine donating resins for trapping iodide. Experiments with several model compounds indicate rapid reaction of iodide. Using model compounds such as vanillin we have demonstrated rapid transformation of iodide to iodo-vanillin by a sulfonamide resin. In these experiments we have monitored both the loss of iodide from solution and the appearance of iodovanillin. Iodovanillin was confirmed by GC/MS analysis. The results of one experiment that demonstrates the rapid kinetics of this process are shown below. This experiment was conducted with 10.0 mM NaI and 13.0 mM vanillin in a $NaHCO_3$ buffered solution. The reaction was initiated by addition of 50 mg of a sulfononamide resin with approximate 1 meq/gram (wet) of active chlorine.

We are in the process of conducting experiments with these resins in the presence of complex NOM.

In order to demonstrate the presence of iodine in the treated organic matter we have pyrolyzed (400-700C) iodine treated NOM, and examined volatile and semivolatile products. The results of this study indicate that bound iodine is released from the pyrolyzed organic matter predominantly as methyl iodide. Trace quantities of ethyl iodide were detected. A total ion chromatogram generated by pyrolysis of 0.9 mg of lignin treated with iodine (~40 μmoles of iodine per mg of lignin) is shown in Figure 1.3.3a. This pyrogram is dominated by methyl iodide, which elutes at scan 350. A single ion chromatogram (142 m/e) is presented for the sample in Figure 1.3.3b. Pyrolysis leaves most of the starting material as an organic residue.

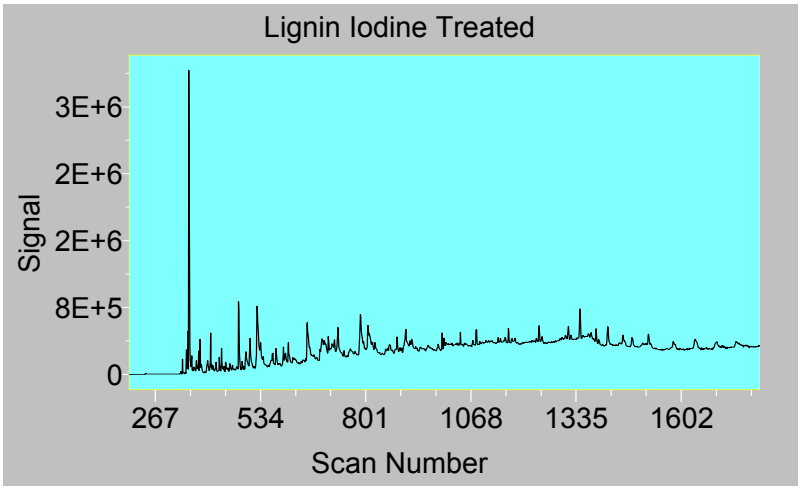

Figure 1.3.3a: Chromatogram of pyrolysis products of lignin that was allowed to react with iodine in aqueous solution.

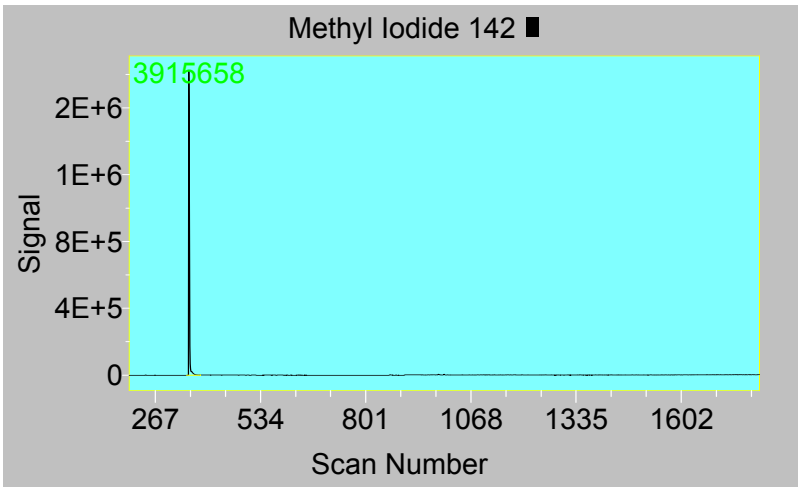

Figure 1.3.3b: Specifc ion chromatogram (142 m/e) corresponding the molecular weight of methyl iodide. The integrated peak area is shown in the figure.

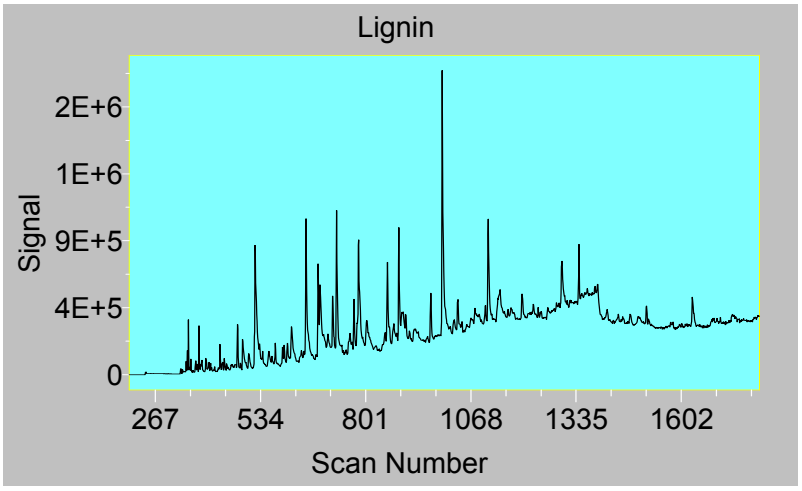

Figure 1.3.4a: Pyrogram of lignin that was not exposed to iodine treatment.

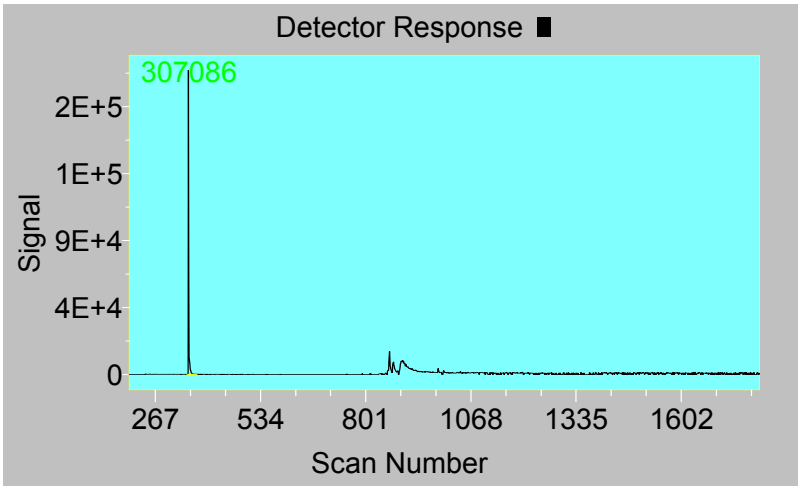

Figure 1.3.4b. Single ion chromatogram that indicates the presence of methyl iodide in untreated lignin.

In comparison, the chromatogram of pyrolysis products for untreated lignin had numerous peaks corresponding to phenolic compounds (Figure 1.3.4a). These peaks are largely missing from the iodine treated sample. It is interesting that methyl iodide can be identified in the untreated lignin, however, its abundance as illustrated by the integrated area of the 142 (m/e) peak is much lower (Figure 1.3.4b).

Methyl iodide can easily be hydrolyzed to methanol and sodium hydroxide. We propose that this reaction may be conducted on a macroporous strongly basic anion exchange resin (in hydroxide form). The results of this process would leave the iodide associated with the anion exchange resin, from which it could be recovered for further processing. One can envision a reaction such as:

$$CH_3I + (Pol \sim N(CH_3)_3{}^+OH^-)_{solid} \rightarrow (Pol \sim N(CH_3)_3{}^+I^-)_{solid} + CH_3OH$$

The hydrolysis process leaves iodide associated with the anion exchange resin from which it could be eluted with a strong base such as sodium or ammonium hydroxide. Many suitable resin are commercially available for testing. Pyrolysis may therefore present a useful approach for recovering and concentrating sequestered iodine for further treatment such as transmutation or incorporation into a ceramic.

Fluorapatite Waste Forms (Task 16). Fluorapatite, fluorinated calcium phosphate, has been identified as a potential matrix for the entombment of the zirconium fluoride fission product waste stream from the proposed FLEX process. If the efficacy of fluorapatite-based waste-storage can be demonstrated, then new and potentially more-efficient options for handling and separating high-level wastes, based on fluoride-salt extraction, will become feasible. This task is a dual-path research project to develop a process to fabricate a synthetic fluorapatite waste form for the ZrF_4, FP waste stream, characterize the waste form, examine its performance under environmental conditions, and correlate the behavior of the waste form with natural analogs. Characterization of the material will be accomplished through probing the molecular-scale electronic and geometric structure of the materials in order to relate them to macroscopic properties, with the goal of developing techniques to evaluate and predict the performance of different waste-form materials. Time and funding permitting, other waste forms for the zirconium fluoride, fission product salt waste stream will be examined and benchmarked against the fluorapatite matrix baseline.

The primary efforts by the two Chemistry M.S. students on this project have been to obtain baseline spectroscopic and imaging data (see Highlights) on pure samples of commercial hydroxyapatite and natural fluorapatite. The goals of these efforts are two-fold: (1) to have fundamental data with which to compare physically and chemically modified materials relevant to waste-storage issues; and (2) to provide substantial training opportunities for the graduate students. A detailed analysis of the measured data also was begun during the reporting period.

Last quarter discussions were held that led to plans for physically and chemically preparing

samples of hydroxyapatite and fluorapatite "loaded" with surrogate waste materials, such as transition metals and compounds. These plans were developed with the goal of initiating efforts along these lines during summer 2003.

TRANSMUTATION SCIENCES

Niobium Cavity Fabrication Optimization (Task 2). Multipacting is one of the major loss mechanisms in rf superconductivity cavities for accelerators. This loss mechanism limits the maximum amount of energy/power supported by the cavities. Optimal designs have been identified in others' studies. In practice, these designs are not easily manufactured. Chemical etching processes used to polish the cavity walls result in a nonuniform surface etch. A nonuniform surface etch will leave some unclean areas with contaminants and micron size particles. These significantly affect mutipacting. Further, a nonuniform etch will leave areas with damaged grain structure, which is not good for superconducting properties. Typically, the depth of chemical polishing etch ranges between 10 to 150 microns.

It is the purpose of this study to experimentally model the fluid flow resulting in the chemical etching of niobium cavities with the aid of a baffle. The current etching process with baffles does not uniformly etch the cavity surface. Multiple cavity cell geometries are being investigated. Optimization techniques will be applied in search of the chemical etching processes that will lead to cavity walls with near ideal properties.

LBE Corrosion of Steel (Task 3). The goal of this task is to achieve a basic understanding of corrosion of steels by Lead Bismuth Eutectic (LBE). There have been previous studies of LBE, especially by the Russians, who have over 80 reactor-years experience with LBE coolant in their Alpha-class submarine reactors. The Russians found that the presence of small amounts (ppm) of oxygen in the LBE significantly reduced corrosion. However, a fundamental understanding and verification of its role in the corrosion of steels is still very incomplete.

We are carrying out a program of post-experiment testing and analysis on steel samples that have been in intimate contact with LBE. We have employed surface analysis techniques, including Scanning Electron Microscopy (SEM), Energy Dispersive X-Ray (EDAX) spectroscopy, and X-ray Photoelectron Spectrometry (XPS), and laser Raman. These techniques, applied to the steel surface, have probed the surface morphology, elemental analysis and oxidation states as a function of position. The measurements were made using the facilities at UNLV. Chemical alterations and resulting chemical species are studied at the steel surface. We plan to use powder X-ray diffraction in the near future. In addition to these well-established laboratory-based instrumentation approaches at UNLV, we have begun to use a state-of-the-art synchrotron-based spectroscopy and microscopy technique, the X-ray fluorescence microprobe at the Advanced Light Source, at Lawrence Berkeley National Laboratory. We are characterizing spectroscopically the stainless steel before and after interaction with LBE to determine their composition, including minor components such as chromium and nickel. The research moves toward establishing a rigorous experimental database of experimental measurements of LBE and its reactions with steels. Such a database can be used by DOE scientists and engineers in engineering efforts to control, avoid, and/or minimize the effect of corrosion of steels by LBE.

Environment-induced Degradation of Materials (Task 4). During the past two years of this project, the primary effort was focused on evaluating the effect of hydrogen on the cracking behavior of candidate target materials namely, Alloys EP-823, HT-9 and 422 in aqueous environments of different pH values at ambient and elevated temperatures. More recently, emphasis is being placed to evaluate the cracking behavior of these materials in molten lead-bismuth eutectic (LBE) environment at much higher testing temperatures so as to compare the cracking susceptibility in environments containing molten metals and aqueous solutions, respectively.

The most recent tests to evaluate the cracking susceptibility were primarily based on two state-of-the-art techniques known as constant-load and slow-strain-rate (SSR) methods. Simultaneously, efforts were made to determine the localized corrosion (pitting and crevice corrosion) behavior in similar aqueous environments at ambient and elevated temperatures using electrochemical polarization techniques. However, these techniques cannot be applied to LBE environment. Therefore, the work scope described in the original proposal has been modified to include additional testing methods to suit the high-temperature LBE environment. Although, testing still will be continued to complete the original matrix involving all three alloys in aqueous environments using constant-load, SSR, and polarization techniques, future testing will be performed in both aqueous and LBE environments using self-loaded specimens such as C-Ring and U-Bend stress-corrosion-cracking (SCC) test specimens.

In addition to this corrosion testing, significant efforts will be made to evaluate the crack-growth behavior of radiation-hardened target materials using sub-size compact tension (CT) specimens. The test materials will undergo appropriate thermal treatments prior to their testing. All tested specimens will be examined metallographically. Further, the scanning electron microscope (SEM) will be used to determine the extent and nature of cracking in the tested specimens. The thrust of this overall testing program is to evaluate the environmental and radiation effects on the cracking behavior of candidate target materials.

LBE Corrosion Modeling (Task 5). This project combines chemical kinetics and hydrodynamics in target and test-loop lead-bismuth eutectic (LBE) systems to model system corrosion effects. The goal is to produce a predicative tool that can be validated with corrosion test data, used to systematically design tests and interpret the results, and provide guidance for optimization in LBE system designs. The task includes two subtasks. The first subtask is to try to develop the necessary predictive tools to be able to predict the levels of oxygen and corrosion products close to the boundary layer through the use of Computational Fluid Dynamics (CFD) modeling. The second subtask is to predict the kinetics in the corrosion process between the LBE and structural materials by incorporating pertinent information from the first subtask.

Overall Corrosion Modeling:

The model is a 5m long rectangular loop with a circular cross-section. Because of the non-symmetry, and due to the active participation of the secondary flows due to the elbows present in the rectangular loop model, the geometry is considered as a 3-D model.

A momentum source has been introduced in the model to account for the pump in the loop. The model has been tested for both laminar and turbulent flow regimes the Reynolds' number being 2000 for the laminar flow and 200,000 for the turbulent flow. The diffusion in the lateral direction for laminar flow is more predominant than for the turbulent flow.

Comparison of Analytical and Simulation Models:

For the purpose of benchmarking the present package, the concentration/precipitation zones obtained from the package should be in tune with the analytical results. When the regions of maximum corrosion and precipitation are compared, they fall in the same zone for both the analytical and simulated models. The reason for a larger concentration flux in the case of turbulent flow than for the laminar flow can be explained by the concept of higher lateral diffusion in the latter case. Because of the higher concentration diffusion in the laminar regime than in the turbulent regime, the concentration difference between the wall and the outermost layer of cells in the former case is lesser for the former case than the latter case

A grid independency check has been conducted to ensure that the results from the runs are not grid dependent. The check has been performed for both the laminar and turbulent flows. To do this test, three different grid sizes have been modeled and the results compared for all the three models. The variable of comparison used is the concentration flux along the loop length.

Local Corrosion Modeling:

One of the important factors affecting corrosion rate is concentration gradient, especially when corrosion happens in the environment which involved complicated flow movement. Vortexes and circulations disturb the formation of boundary layer. Consequently, theoretical estimation of mass transfer phenomenon is not applicable and more uncertainties need to be considered in those kinds of situations. Flow pattern decides the way how species is washed from the wall and diffuses into bulk region. In the code, concentration gradient at wall is calculated according to expression $\frac{C_{wall} - C_{wall-1}}{\Delta y}$. In the light of unsteady nature of flow, at each cross section, concentration gradients on upper and bottom wall are taken average to show general idea of how species is transported at near-wall region along the distance to inlet.

Work is basically carried out with the parametric study of expansion ratio. Different combinations show how those factors affect species transportation. To find out the effects on mass transfer brought in by expansion ratio, three ratios were chosen to look at: 3, 6 and 10. We have found that, at each expansion ratio, higher Reynolds Number generally yields higher concentration gradient. When Reynolds Number is very low, like around 10, concentration gradient varies smoothly from inlet to a certain distance and reaches its maximum value. After that point, it remains at the same value. While Reynolds Number goes up, flow becomes unsteady. Instead of smooth curve, lines start oscillating and contain numbers of peaks along X coordinate. It is because of vortexes and circulations disturb the formation of boundary layer.

It is also can be observed that for the same expansion ratio, maximum of concentration gradient for those relatively high Reynolds Numbers occurs almost at same distance to inlet, while the

value of maximum differs in the same order. With the increasing of expansion ratio, the distance to inlet where biggest concentration gradient occurs is pushed downstream. Figure 1.3.5 depicts the trend between peak location and expansion ratio.

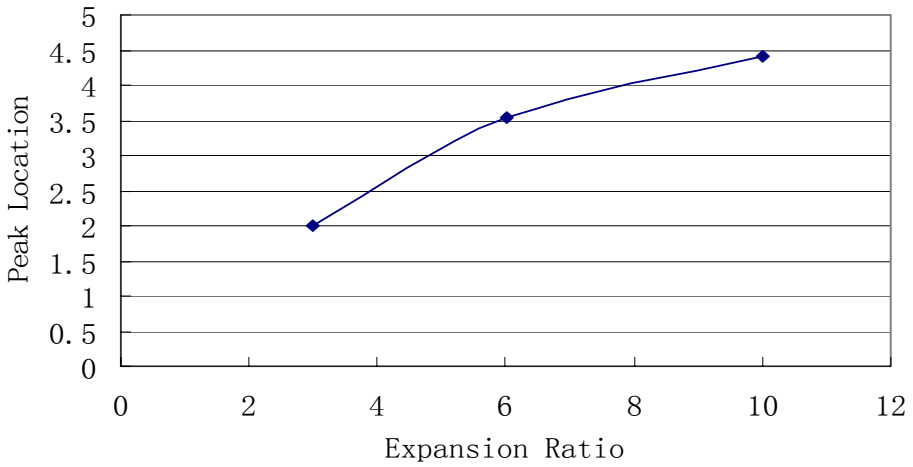

Figure 1.3.5. Peak Locations at Different Expansion Ratios

Neutron Multiplicity (Task 6). The goals of this task are to measure the neutron leakage from 15, 20 and 40-cm diameter Pb-Bi / Pb targets and to compare these empirical measurements with MCNPX results. These measurements are essential in validating and benchmarking MCNPX modeling results of target materials. The neutron leakage measurements should provide a systematic set of precision data that will enable direct comparison with code calculations. Two detector systems, which employ independent technologies, are in fabrication. Comparisons of results obtained from both should remove many uncertainties and permit the derivation of relative measurements in the few percent range at the 95% Confidence Level (CL). A 60 detector element ^{3}He tube based system and a prototype neutron sensitive glass fiber-based system were designed during Yr-1 of this study. The glass fiber detector prototype is complete and ready to test in upcoming target experiments at LANCSE. The 60 element ^{3}He based, target monitoring system is in final design and initial fabrication stages. MCNPX models of the ^{3}He system have been developed and will be integrated with target models. Models of the glass fiber detectors have been developed and used for developing July 2002 LANSCE target experiments.

Dose Conversion Coefficients (Task 7). A research consortium comprised of representatives from several universities and national laboratories has been established as part of this task to generate internal and external dose conversion coefficients (DCC) for radionuclides produced in spallation neutron sources. Information obtained from this study will be used to support the siting and licensing of future accelerator-driven nuclear initiatives within the U.S. Department of Energy complex, including the Spallation Neutron Source (SNS) project. Determination of these coefficients will also fill data gaps for several hundred radionuclides that exist in Federal Guide Report No. 11 and in Publications 68 and 72 of the International Commission on Radiological Protection (ICRP).

Properties of Alloy EP-823 (Task 10). The purpose of this project is to evaluate the elevated temperature tensile properties of Alloy EP-823, a leading target material for accelerator-driven waste transmutation applications. This alloy has been proven to be an excellent structural material to contain the lead-bismuth-eutectic (LBE) nuclear coolant needed for fast spectrum operations. Very little data exist in the open literature on the tensile properties of this alloy. The test material will be thermally treated prior to the evaluation of its tensile properties at temperatures relevant to the transmutation applications. The deformation characteristics of tensile specimens, upon completion of testing, will be evaluated by surface analytical techniques using scanning electron microscopy (SEM) and transmission electron microscopy (TEM). The overall results will lead to the development of a mechanistic understanding of the elevated-temperature deformation processes in this alloy as a function of thermal treatment. The resultant data may also provide guidance in developing future target materials possessing the improved metallurgical properties, and enhanced LBE corrosion resistance.

Radiation Transport Modeling of Beam-Target Experiments (Task 12). The AFCI program will rely on the use of accurate calculations and simulations of criticality and shielding for the separation process of the long-lived isotopes that present a significant safety hazard in commercial spent fuel. To help design and verify the safety of the separation process, the neutronics code MCNPX will be used to model the distribution of neutron flux within the fuel blanket and to determine the neutron multiplication, k_{eff}. However, the cross section libraries and computational methods used by MCNPX at these neutron energies still have some uncertainty and will require validation.

Over the past two years, the faculty and students on this project have worked with researchers at LANL and the Idaho Accelerator Center to use MCNPX in support of the work on the Transmutation of Nuclear Waste. During this effort, our students have traveled to LANL and the IAC to support projects on neutron production using both proton and electron accelerators. A parallel cluster of 20 computers has been assembled at UNLV to support these MCNPX simulations.

Currently MCNPX relies on a hand created input deck, which can be time consuming to produce and prone to errors. One way to solve this problem is to create a graphical user interface (GUI) to help the user create the input deck. Also, to achieve accurate results in a short period of time there is a need to increase the efficiency of the parallel version of MCNPX. We propose to involve UNLV students and faculty in this endeavor to create a GUI, to increase the speed of MCNPX on parallel clusters of computers, and to continue application of MCNPX to solve practical AFCI problems.

Oxygen Sensing in LBE (Task 13). Although liquid lead-bismuth eutectic (LBE) is a good candidate as a coolant in fast nuclear systems, it is known to be very corrosive to stainless steel, the material of the carrying tubes and containers. Such a corrosion problem can be prevented by producing and maintaining a protective oxide layer on the exposed surface of stainless steel. The proper formation of this oxide layer critically depends on the accurate measurement and control of the oxygen concentration in liquid LBE. YSZ (Yttria Stabilized Zirconia) oxygen sensors, using molten bismuth saturated with oxygen as the reference, have been utilized to accurately measure the concentration of oxygen dissolved in LBE.

A new experimental apparatus with several important improvements to an older version at LANL is under development at UNLV. The proposed specific aims of the task are: (1) To complete and fully test the new oxygen control and measurement apparatus; (2) To continue the sensor calibration by using our new set-up at higher temperature ranges (350 ^{0}C to 700 ^{0}C); (3) To employ a more precise and easier H_2/H_2O steam injection strategy for oxygen control instead of previous method of direct injection of O_2; (4) To simulate the dissolved oxygen concentration distribution in the liquid LBE of our system by using FEMLAB or other software (ABAQUS/FLUENT). The results obtained from the simulations will be used to cross-check and cross-validate with the experimental data; (5) To determine oxygen dissolving rates under various conditions including changing temperatures and inlet O_2 supply; and, (6) To determine the diffusion coefficient of O_2 in liquid LBE under different temperatures through theoretical modeling and experimental measurement.

Positron Annihilation Spectroscopy (Task 14). The purpose of this collaborative research project involving UNLV, ISU, and LANL is to evaluate the feasibility of determining residual stresses in cold-worked, plastically-deformed (bent), and welded materials using a nondestructive method based on positron annihilation spectroscopy (PAS). This technique uses γ-rays from a small MeV electron Linac to generate positrons inside the sample via pair production. This method is known to have capabilities of characterizing defects in thick specimens that could not be accomplished by conventional positron technique or other nondestructive methods. The generated data will be compared to those obtained by other methods such as neutron diffraction and X-ray diffraction (for thin specimens), and ring-core (destructive-for thick specimens) methods. During the initial phase, residual stresses induced in experimental heats of austenitic Type 304L stainless steel, and martensitic Alloy EP-823 have been determined by X-ray diffraction, PAS and ring-core techniques. More recently, efforts are ongoing to include Alloy HT-9, another martensitic stainless steel to perform similar measurements on this alloy using all four techniques. Later, irradiated materials may be evaluated. Low-level radiation will be induced in the test specimens at the ISU, followed by residual stress measurements using the PAS method.